Fatigue Response of Ti/APC-2 Nanocomposite Laminate Prosthesis

Ming-Hwa R. Jen*, Che-Kai Chang, Jing-Guan Chen and Bo-Cyuan Lin

Dept. of Mechanical and Electro-Mechanical Engineering, National Sun Yat-Sen University, Kaohsiung 80424, Taiwan.

*Corresponding Author: Ming-Hwa R. Jen; E-mail: jmhr@mail.nsysu.edu.tw

Abstract: The post mechanical behavior of Ti/APC-2 hybrid nanocomposite laminate prosthesis after low velocity impact was investigated. The three layered Ti/APC-2/Ti cross-ply nanocomposite laminates were fabricated according to the modified the diaphragm curing process based on the previous experience. Each sample, L×W×t=240mm×25mm×1.55mm, was first subjected to free drop of a rigid steel ball (diameter=12.7mm) of 1m and 2m high. Then, the samples were due to static tensile tests at room temperature to measure their residual ultimate strength and longitudinal stiffness as the base-line data for constant stress amplitude tension-tension cyclic tests. The corresponding S-N curve, fatigue strength and life were obtained. Also, the mechanism of damage by impact and failure of separation were observed. The mechanical properties do not reduce significantly due to low-velocity impact, even if the damage area is obviously large for 2m high free drop. Similarly, the fatigue resistance of impacted samples does not lose much. It is mainly attributed to the damage only occurs on the surface of impacted samples with little influence inside the laminates by low-velocity impact. It can be concluded that the enhancement by nanoparticles and superior bonding capability of matrix PEEK with Ti sheets take the responsibility of improvement of mechanical responses.

[Ming-Hwa R. Jen, Che-Kai Chang, Jing-Guan Chen and Bo-Cyuan Lin. Fatigue Response of Ti/APC-2 Nanocomposite Laminate Prosthesis. Life Science Journal. 2012; 9(2):178-184] (ISSN:1097-8135). http://www.lifesciencesite.com. 30

Keywords: Ti alloy; Gr/PEEK(APC-2); Nano; Composite; Impact; Tension; Fatigue

1. Introduction

Osteo-arthritis affects joints between bones due to the growth of small lumps of bone on the contacting surfaces of the joints. This prevents the joints from sliding in the usual manner, causing excruciating pain during movement^[1]. Replacing a natural joint with an artificial joint offers good potential to alleviate the problem. In hip joint replacement operations, the head of the femur is sectioned-off, and the soft marrow is removed to create a hollow intra-medullar cavity through the centre of the femur shaft. An artificial implant (mainly comprising of a long stem and a head) is then glued into the femoral cavity. The implant head fits into the acetabular socket of the hip bone. The critical mechanical property requirements of the implant material include (but are not limited to) high specific bending stiffness, high bending stiffness comparable to that of the surrounding cortical bone, biocompatibility, corrosion resistance and high endurance limit. It is noteworthy that the loads on a typical joint fluctuate approximately a million times a year^[2].

Titanium (Ti) and its alloys have been utilized in medical practice, for they have high-strength/density ratios, excellent corrosion resistance to biological environments, and strong adhesion to bone tissue^[3].

A lower modulus implant material would result

in the construction of a more biomechanically compatible prosthesis. In this respect, carbon and aramid fiber reinforced polymer matrix (such as polyether ether ketone – PEEK) composite materials are gaining importance, because they offer the potential for implants with tailor-made stiffness in contrast to metals. They possess superior biomechanical properties, such as better fatigue strength, chemical resistance, environmental stability, and resistance to sterilization by c-radiation and biocompatibility.

Owing to the brittleness of thermosetting matrix resulted by cross-linking, the epoxy resins and epoxy-based fiber composites are susceptible to impact damage. Thermoplastics, having greater toughness, are considered to have the potential for alleviating this problem^[7].

For example, during the last ten years, the Defence Research Establishment (DREV) has been studying the application of composite materials for generic anti-tank recoilless gun^[8]. To achieve the desired weight reduction, a graphite-epoxy composite material was used to manufacture the gun tube and venturi. Although the ballistic viability of such a design was well proven during tests and evaluations, one major concern that remains is sensitivity of the thermoset resin (epoxy) to the low-level damage accumulation due to a mixture of normal loading and rough handling in the field. Such damage is generally

barely visible, and it is therefore important to develop an adequate NDT inspection technique to permit testing as close as possible to an operational environment.

Although damage inflicted by low-velocity impact appears quite complicated, the major failure modes include only matrix cracking, delamination, and fiber breakage^[9]. As pointed out by Sun and Rechak^[10], the delamination mode of failure is induced by matrix cracks which occur prior to other failure modes. Thus, suppression of matrix cracking will suppress delamination. It is conceivable that the use of tougher matrices will yield composites that are more resistant to impact damage.

Except for the degree of damage, the plate specimens did not differ from beam specimens in failure modes or impact tolerance properties^[11], i.e., no plate size effect. The postimpact load-carrying capability of a composite laminate is of prime concern to the design engineer. After a tool-drop type accident where no damage is visible from the surface, the structure is still expected to carry the full spectrum of loading. However, it may be wrong of overestimation. In all cases the residual strength decreased as the impact velocity increased. From the results^[10] the tough matrix composites may provide excellent impact resistance properties at low-impact velocities. However, beyond a certain threshold velocity, the use of tough matrix materials may result in more laminate tensile and flexural strength reduction than that of brittle matrix materials.

Additionally, the PEEK composites have significantly lower contact rigidity, i.e., for a given contact force the resulting indentation in the PEEK composites would be larger, yielding a larger contact area, and, therefore, a low contact pressure. A larger contact area with lower pressure will reduce the transverse shear stress concentration and thus minimize local matrix cracking.

From the above-mentioned it is clear that little reduction in strength in the tough PEEK composite laminates prior to the low velocity, i.e., $\leq 25 \text{m/s}$. Beyond this point the matrix damage occurred and substantial fiber breakage followed. That explains the sudden drop of strength in PEEK laminates when impacted at velocities higher than 25 m/s.

Based on the knowledge of merits and disadvantages of PEEK composites within the scope of low velocity we fabricated the Ti/APC-2 hybrid nanocomposite laminates to investigate their resistance and mechanical properties by tensile and fatigue tests after free drop of a steel ball at 1m and 2m high. Nejad^[12] investigated the stresses in the sphere rests on a rigid plane horizontal surface. The related surface treatment and adding nanoparticles are stated as follows.

Anodic method is a commonly used surface treatment, however, the bonding capability of polymer composites to titanium thin plates is still a problem. In order to improve the interfacial bonding capability, Ramani et al.^[13] found the chromic acid anodic method was excellent. Chromic acid anodic oxidation produced an oxide layer of thickness 40~80 nm for the 5 V and 10V treatments^[14]. Ibrahim et. al.^[15] investigated the influence of resin-tags on shear-bond strength of butanol-based adhesives.

In recent years, inorganic nanoparticles filled polymer composites have attracted attention because the filler/matrix interface in these composites might constitute a great area and influence the properties of composites at rather low filler concentration^[16]. Herein, our concern is focused on an engineering application, i.e., dispersing SiO₂ nanoparticles 1wt% optimally on the interfaces of APC-2 composite laminates to improve the mechanical properties of samples due to static and cyclic loadings as an extension of previous work^[17].

From the bonding of Ti with APC-2 by the modified diaphragm curing process, Ti/APC-2 hybrid nanocomposite laminates were successfully fabricated. The mechanical properties of samples subjected to tensile and cyclic tests at room temperature after low velocity impact were obtained. The failure mechanisms were observed.

2. Experimental

The twelve-inch wide prepregs of Carbon/PEEK (Cytec Industries Inc., USA) unidirectional plies were cut and stacked into cross-ply [0/90]_s laminates. The nanoparticles SiO₂ (Nanostructured & Amorphous Materials, Inc. USA) possessed the average diameter 15±5 nm, specific surface area 160±20 m²/g, spherical crystallographic and amorphous powder. The optimal amount of SiO₂ was found 1% by wt. of laminates. The grade 1 (H: 0.015%, O: 0.18%, N: 0.03%, Fe: 0.2%, C: 0.08%) Ti sheets, supplied by Kobe Steel Ltd (Japan), were 0.5mm thick after rolled, heated and flattened with scratch brushing. The ultimate tensile strength of Ti is 353MPa, and modulus of elasticity 109GPa.

Prior to lamination, the slimmed Ti alloy sheets were subjected to pretreatment in order to create the tough bonding with APC-2 prepregs. After a series of tests, the surface treatment by chromic acid anodic method of electro-plating was found better as demonstrated by the results of tensile tests. After anodic processing, the thickness of oxide coating film was about 40~80nm. The anodic oxide coating was observed uniform by SEM, and the composition of coating consisting of TiO₂ by EDS.

The APC-2 prepregs were sandwiched with the

Ti alloy sheets to produce Ti/APC-2 hybrid three-layered laminated composites. The modified diaphragm curing process was adopted [9]. The hybrid composite specimen was a plate of $240 \text{mm}(L) \times 25 \text{mm}(W) \times 1.55 \text{mm}(t)$ as shown in Figure 1.

The samples were divided into three groups, such as virgin, due to 1m high free drop, and 2m high free drop. The steel ball was 12.7mm in diameter and 8.3g of weight. The velocities at the contact of sample surface was 4.41m/s for 1m high, and 6.28m/s for 2m high, respectively.

An MTS-810 servohydraulic computer-controlled dynamic material testing machine was used to conduct the tensile test and constant stress amplitude T-T cyclic test with stress ratio=0.1, frequency=5HZ, sinusoidal wave form under load-controlled mode at room temperature after the free drop of a steel ball.

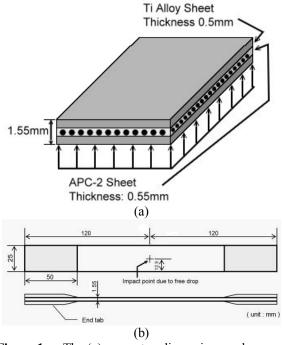


Figure 1. The (a) geometry, dimensions and supported conditions of Ti/APC-2 cross-ply nanocomposite laminate, (b) due to impact of free drop by steel ball.

3. Results

The mechanical properties of Ti/APC-2 cross-ply laminates were listed in Table 1(a) for virgin samples, (b) for samples due to 1m high free drop, and (c) for samples due to 2m high free drop. Also, the mechanical properties of Ti/APC-2 cross-ply nanocomposite laminates were in Table 2(a) for virgin specimens, (b) for specimens after a free

drop at 1m high, and (c) for specimens after a free drop at 2m high, respectively. The stress-strain curves of Ti/APC-2 nanocomposite laminates after a 1m high free drop impact was shown in Figure 2. for example. It should be paid attention that there is a kink angle, i.e., knee, in stress-strain curves of hybrid laminates, such as Al/APC-2 and Ti/APC-2 W/WO nanoparticles.

Table 1 The mechanical properties of Ti/APC-2 cross-ply laminates (a) virgin samples, (b) samples after a free drop impact at 1m high, and (c) samples after a free drop impact at 2m high.

$ \begin{array}{c ccccccccccccccccccccccccccccccccccc$		
$ \begin{array}{c ccccccccccccccccccccccccccccccccccc$		
$\begin{tabular}{ c c c c c c c c c c c c c c c c c c c$	Longitudinal Stiffness	
$ \begin{array}{c ccccccccccccccccccccccccccccccccccc$	cant	
$\begin{array}{c ccccccccccccccccccccccccccccccccccc$	11s	
$\begin{array}{c ccccccccccccccccccccccccccccccccccc$	GPa)	
$\begin{array}{c ccccccccccccccccccccccccccccccccccc$	0.38	
Average 24.66±0.58 636.3±15.01 0.017±0 101.86±0.82 29.66 Notes: $E_{11i}(Tangent\ Modulus): 0.0005 \le 0.00165$ $E_{11s}(Secant\ Modulus): 0.007 \le 0.013$	9.23	
Notes: $ \begin{array}{c} E_{1i}(Tangent\ Modulus):\ 0.0005 \le \epsilon \le 0.00165 \\ E_{1ls}(Secant\ Modulus):\ 0.007 \le \epsilon \le 0.013 \end{array} $	9.39	
Notes: E _{11s} (Secant Modulus) : 0.007≤ε≤0.013 (b)	6±0.63	
<u> </u>	Longitudinal Stiffness	
	ecant	
No. (KN) (MPa) Strain tangent E _{11i} E	E11s	
(GPa) (C	GPa)	

	T. T	*****		Longitudinal Stiffness	
Sample	Ultimate Load	Ultimate Strength	Maximum	Initial	Secant
No.	(KN)	(MPa)	Strain	tangent E_{11i}	E_{11s}
				(GPa)	(GPa)
1	22.57	582.45	0.0171	101.81	26.83
2	23.24	599.74	0.0178	94.70	26.98
3	23.34	602.32	0.0182	93.98	25.42
Average	23.05±0.42	594.84±10.8	0.018±0.001	96.83±4.33	26.41±0.86

 $Notes: \begin{array}{l} E_{11i}(Tangent\ Modulus) : 0.0005 \!\! \leq \!\! \epsilon \!\! \leq \!\! 0.00165 \\ E_{11s}(Secant\ Modulus) : 0.007 \!\! \leq \!\! \epsilon \!\! \leq \!\! 0.013 \end{array}$

			(c)		
				Longitudinal Stiffness	
Sample	Ultimate Load	Ultimate Strength	Maximum	Initial tangent	Secant
No	(KN)	(MPa)	Strain	E_{11i}	E_{11s}
				(GPa)	(GPa)
1	22.84	589.42	0.0153	105.03	30.06
2	22.38	577.55	0.0151	103.64	29.73
3	23.06	595.10	0.0159	105.37	29.56
Average	22.76±0.35	587.36±8.96	0.015±0	104.68±0.92	29.78±0.26

 $\begin{aligned} \text{Notes:} \quad & \frac{E_{11i}(Tangent\ Modulus) \ \colon 0.0005 \!\!\le\!\! \epsilon \!\!\le\!\! 0.00165}{E_{11s}(Secant\ Modulus) \ \colon 0.007 \!\!\le\!\! \epsilon \!\!\le\!\! 0.013} \end{aligned}$

Table 2 The mechanical properties of Ti/APC-2 cross-ply nanocomposite laminates (a) virgin samples, (b) samples after a free drop impact at 1m high, and (c) samples after a free drop impact at 2m high.

(a)						
	Ultimate Load (KN)	Ultimate Strength (MPa)	Maximum Strain	Longitudinal Stiffness		
Sample No.				Initial	Secant	
				tangent E_{11i}	E_{11s}	
				(GPa)	(GPa)	
1	24.96	644.13	0.0160	95.28	31.89	
2	25.37	654.71	0.0174	98.95	29.50	
3	25.68	662.71	0.0175	99.39	30.60	
Average	25.34±0.36	653.85±9.32	0.017±0.001	97.87±2.26	30.66±1.2	
Notes:	$\begin{split} E_{11i}(&Tangent\ Modulus):\ 0.0005 \underline{\le} \epsilon \underline{\le} 0.00165 \\ E_{11s}(&Secant\ Modulus):\ 0.007 \underline{\le} \epsilon \underline{\le} 0.013 \end{split}$					

			(b)		
	Ultimate Load (KN)	Ultimate Strength (MPa)	Maximum Strain	Longitudinal Stiffness	
Sample				Initial	Secant
No.				tangent E_{11i}	E_{11s}
				(GPa)	(GPa)
1	26.26	674.98	0.0185	94.39	30.30
2	25.52	655.96	0.0187	94.14	28.25
3	25.41	655.74	0.0184	100.65	29.15
Average	25.73±0.46	662.23±11.05	0.019±0.0002	96.39±3.69	29.23±1.03
Notes: E _{11i} (Tangent Modulus) : 0.0005≤ε≤0.00165					

$E_{11s}(Secant Modulus) \cdot 0.00/\leq \epsilon \leq 0.013$						
	(c)					
	Ultimate Load (KN)	Ultimate Strength (MPa)	Maximum Strain	Longitudinal Stiffness		
Sample No				Initial	Secant	
				tangent E_{11i}	E_{11s}	
				(GPa)	(GPa)	
1	22.03	568.52	0.0162	99.19	26.54	
2	22.17	572.13	0.0157	99.49	27.58	
3	23.05	594.84	0.0163	102.50	28.30	
Average	22.42±0.55	578.5±14.27	0.016±0.0003	100.39±1.83	27.47±0.88	
Motor:	E _{11i} (Tangent Modulus) : 0.0005≤ε≤0.00165					

 $E_{11s}(Secant\ Modulus)\ \vdots\ 0.007 \!\!\leq\!\! \epsilon \!\!\leq\!\! 0.013$

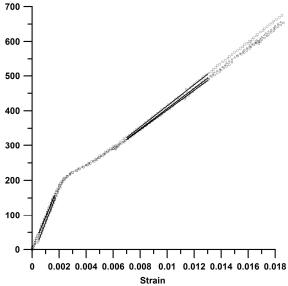


Figure 2. The stress-stain curves for Ti/APC-2 cross-ply nanocomposite laminates after a 1m high free drop impact

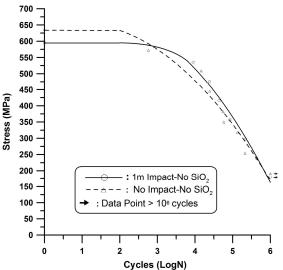


Figure 3. The S-N curves for Ti/APC-2 hybrid composite laminates with and without the impact of 1m high

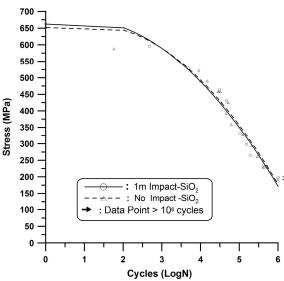


Figure 4. The S-N curves for Ti/APC-2 hybrid nanocomposite laminates with and without the impact of 1m high

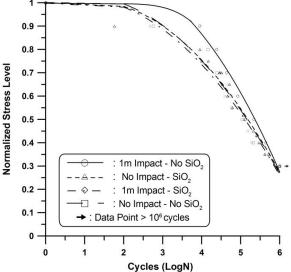


Figure 5. The normalized S-N curves for Ti/APC-2 composite laminates W/WO nanoparticles due to the impact of 1m high or not.

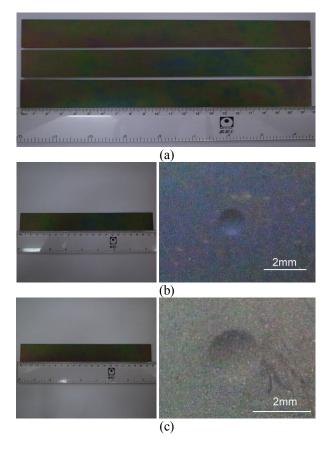


Figure 6. The (a) virgin samples, (b) impacted sample due to 1m high free drop, and (c) impacted sample due to 2m high free drop by a steel ball.

The stress vs. cycles (S-N) curves for Ti/APC-2 cross-ply composite laminates with and without impact of 1m high free drop were illustrated in Figure 3. The S-N curves for Ti/APC-2 cross-ply nanocomposite laminates with and without impact of 1m high free drop were also shown in Figure 4. in contrast. The combined S-N curves, normalized by their corresponding ultimate strength, were presented in Figure 5. The photos of impact indentation were shown in Figure 6.

4. Discussion

It is obvious to see the enhancement of mechanical properties by adding the ${\rm SiO_2}$ nanoparticles in Ti/APC-2 nanocomposite laminates in comparison with the virgin laminates, especially a slight increase of ultimate strength with the stiffness almost unchanged, as depicted in Tables 1(a) and 2(a). However, after the impact of 1m high free drop, the retention of ultimate strength was significantly well, i.e., about 10% more due to the spreading of

nanoparticles in APC-2 laminae in the hybrid laminates when compared with Tables 1(b) and 2(b). Similarly, the longitudinal and secant stiffnesses were also kept unchanged. Referring to the statement in [4] that PEEK composites can't resist the damage due to impact at high velocity, i.e., over 25m/s, nevertheless, the innovative hybrid laminates fabricated herein may have the capability to sustain the impact of high velocity with the improvement of mechanical properties by nanoparticles and metallic sheets. It is the urgent topics for further research.

Generally, it is reasonable that the S-N curves for Ti/APC-2 composite laminates due to impact is lower than that of the same virgin laminates without any impact. However, the S-N curves for Ti/APC-2 nanocomposite laminates with and without impact were very close, i.e., no significant difference. That strongly confirmed the above-mentioned concepts of enhancement and improvement of mechanical and cyclic properties by adding nanoparticles in APC-2 laminae of Ti/APC-2 nanocomposite laminates.

Although the area of impacted surface due to 2m high free drop is greater than that of 1m high free drop, the reduction of mechanical properties of samples impacted by 2m high free drop is not significant as shown in Figure 7. The main reason is that the damage occurred mostly on the surface area with good retention of properties inside the hybrid laminates, i.e., both 1m and 2m high free drop are belonged to low-velocity impact. The velocity of 6.28m/s is near a quarter of high velocity, i.e., the high-velocity impact should be over 25m/s. Additionally, good fatigue resistance of impacted samples due to 2m high free drop can also demonstrate the slight damage occurred in the hybrid laminates. Thus, the problem of high-velocity impact is a worthwhile topics for further research.

5. Conclusion

Ti/APC-2 nanocomposite hybrid laminates were fabricated. The mechanical properties, such as ultimate strength and stiffness, were obtained for virgin samples and impacted samples due to 1m and 2m high free drop. Based on the received properties the cyclic tests were conducted to obtain the S-N curves for three types of laminates.

The mechanical properties do not reduce significantly due to low-velocity impact, even if the damage area is obviously large for 2m high free drop. Similarly, the fatigue resistance of impacted samples does not lose much. It is mainly attributed to the damage only occurs on the surface of impacted samples with little influence inside the laminates by low-velocity impact. It can be concluded that the enhancement by nanoparticles and superior bonding capability of matrix PEEK with Ti sheets take the

responsibility of improvement of mechanical responses.

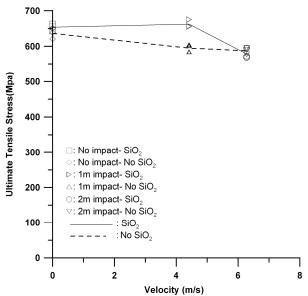


Figure 7. The ultimate strength vs. impact velocity curves for Ti/APC-2 W/WO nanoparticles composite laminates with and without the impact of 1m and 2m high.

References

- 1. Sridhar, I., Adie, P. P., and Ghista, D. N. Optimal design of customised hip prosthesis using fiber reinforced polymer composites. Materials and Design 2010;31:2767-2755.
- Ashby, M.F., Jones, D. R. H. Engineering materials 2: an introduction to microstructures, processing and design. 2nd ed. UK: Butterworth-Heinemann Press; 2000.
- 3. Kawahara, H. Cellular responses to implant materials: biological. physical and chemical factors. Int Dent J 1983;33:350–75.
- 4. Dimitrievska, S, Whitfiled, J., and Hacking S. A., Bureau MN. Novel carbon fiber composite for hip replacement with improved in vitro and in vivo osteointegration. J Biomed Mater Res, Part A 2008;91A(1):37–51.
- Davidson, J. A., Georgette, F. S. State of the art materials for orthopaedic prosthetic devices. In: Proceedings of SME implant manufacturing and material technology conference; December 1986
- 6. Ghista, D. N., Subbaraj, K., and Weiler, P. Custom tailored design specifications of hip prosthetic femoral components for implantation. Human Kinetics Publisher 1985 [Chapter in Biomechanics].

- Dorey, G., Bishop, S. M., and Custis, P. T. On the Impact Performance of Carbon Fiber Laminates with Epoxy and PEEK Matrices. Composites Science and Technology 1985;23:221-237.
- 8. Bolduc, M., and Roy, C. Evaluation of Impact Damage in Composite Materials Using Acoustic Emission. ASTM STP 1993;1156:127-138.
- 9. Joshi, S. P., and Sun, C. T. Impact Induced Fracture in a Laminated Composite. Journal of Composite Materials 1985;19:56-66.
- 10. Sun, C. T., and Rechak, S. Effect of Adhesive Layers on Impact Damage in Composite Laminates. ASTM STP 1988;972:97-123.
- 11. Dan-Jumbo, E., Leewood, A. R., and Sun, C. T. Impact Damage Characteristics of Bismaleimides and Thermoplastic Composite Laminates. ASTM STP 1989;1012:356-372.
- 12. Reza Masoudi Nejad. Stresses in the sphere rests on a rigid plane horizontal surface. Life Science Journal 2011;8(4):290-295.
- 13. Ramani, K., Weidner, W. J., and Kumari, G. Silicon sputtering as a surface treatment to titanium alloy for bonding with PEKEKK. Int. J. Adhesion and Adhesives 1998;18:401-412.
- 14. Ditchek, B. M., Breen, K. R., Sun, T. S., and Venables, J. D. Morphology and composition of titanium adherends prepared for adhesive bonding. In: Proc. 25th Nat. SAMPE Symp. 1980;13–24.
- 15. Ibrahim, Mohamed A., Ragab, H., and El-Badrawy, W. Influence of resin-tags on shear-bond strength of butanol-based adhesives. Life Science Journal, 2010;7(4):105-113.
- Wu, C. L., Zhang, M. Q., Rong, M. Z., and Friedrich, K. Silica nanoparticles filled polypropylene: Effects of particle surface treatment, matrix ductility and particle species on mechanical performance of the composites. Composites Science and Technology 2005;65: 635-645.
- 17. Jen, M. H. R., Sung, Y. C., Chang, C. K., and Hsu, F. C. Fabrication of Ti/APC-2 nanocomposite laminates and their fatigue response at elevated temperature. in: Fifth Int. Conference on Fatigue of Composites, Oct. Nanjing, China 2010;317-325.

3/16/2012